


RESEARCH ARTICLE | MAY 22 2023

# The molten salt synthesis of $ABi_2Ta_2O_9$ ( $A = Ca, Sr, Ba$ ) as photocatalyst material

Usman Ali Rouf; Erna Hastuti; Anton Prasetyo 



AIP Conference Proceedings 2580, 050006 (2023)

<https://doi.org/10.1063/5.0122342>



CrossMark

## Articles You May Be Interested In

CaBi<sub>2</sub>Ta<sub>2</sub>O<sub>9</sub> ferroelectric thin films prepared by pulsed laser deposition

*Appl. Phys. Lett.* (May 2001)

Bright upconversion luminescence and increased T<sub>c</sub> in CaBi<sub>2</sub>Ta<sub>2</sub>O<sub>9</sub>:Er high temperature piezoelectric ceramics

*Journal of Applied Physics* (May 2012)

Effects of BaBi<sub>2</sub>Ta<sub>2</sub>O<sub>9</sub> thin buffer layer on crystallization and electrical properties of CaBi<sub>2</sub>Ta<sub>2</sub>O<sub>9</sub> thin films on Pt-coated silicon

*Journal of Applied Physics* (May 2001)

Downloaded from [http://pubs.aip.org/aip/acp/article-pdf/doi/10.1063/5.0122342/17699478/050006\\_1\\_5.0122342.pdf](http://pubs.aip.org/aip/acp/article-pdf/doi/10.1063/5.0122342/17699478/050006_1_5.0122342.pdf)



## Time to get excited.

Lock-in Amplifiers – from DC to 8.5 GHz



Find out more


# The Molten Salt Synthesis of $ABi_2Ta_2O_9$ ( $A = Ca, Sr, Ba$ ) as Photocatalyst Material

Usman Ali Rouf<sup>1</sup>, Erna Hastuti<sup>2</sup>, and Anton Prasetyo<sup>1, a)</sup>

<sup>1</sup> Department of Chemistry, Faculty of Science and Technology, Universitas Islam Negeri Maulana Malik Ibrahim Malang, Jl. Gajayana 50, Malang, Indonesia, 65144.

<sup>2</sup> Department of Physics, Faculty of Science and Technology, Universitas Islam Negeri Maulana Malik Ibrahim Malang, Jl. Gajayana 50, Malang, Indonesia, 65144.

<sup>a)</sup> Corresponding author: anton@kim.uin-malang.ac.id

**Abstract.** The two-layer member of Aurivillius compound  $ABi_2Ta_2O_9$  ( $A = Ca, Sr, Ba$ ) has been reported can be applied as photocatalyst material. In this research, the compound  $ABi_2Ta_2O_9$  ( $A = Ca, Sr, Ba$ ) was synthesized using the molten salt method and measured photocatalytic activity to degrade methylene blue. Diffractogram samples showed that the compound  $ABi_2Ta_2O_9$  ( $A = Ca, Sr, Ba$ ) was successfully obtained but still found impurities on the samples. Micrograph samples showed that the particle morphology of  $ABi_2Ta_2O_9$  ( $A = Ca, Sr, Ba$ ) was plate-like and found agglomeration in all particles. The calculation using the Kubelka-Munk equation exhibited that  $CaBi_2Ta_2O_9$ ,  $SrBi_2Ta_2O_9$ ,  $BaBi_2Ta_2O_9$  sequentially have bandgap energy of 3.51, 3.21, and 2.44 eV. The degradation test results of methylene blue solution show that  $CaBi_2Ta_2O_9$ ,  $SrBi_2Ta_2O_9$ , and  $BaBi_2Ta_2O_9$  materials can degrade sequentially by 14.44, 24.23, and 15.99 % for 80 minutes.

## INTRODUCTION

Ferroelectric properties of a material are reported to increase photocatalyst activity due to delayed electron-hole recombination rates [1]. It is well known that the Aurivillius compound has good ferroelectric properties; therefore, the opportunity application of Aurivillius compound as photocatalyst material has attracted more attention [2]. The Aurivillius compounds have a general formula  $(A_{n-1}B_nO_{3n+1})^{2-}(Bi_2O_2)^{2+}$ , and the pseudo-perovskite layer  $(A_{n-1}B_nO_{3n+1})^{2-}$  arranged alternately with bismuth layers  $(Bi_2O_2)$  with  $n$  represents the number of pseudo-perovskite layers.  $A$ -site cations were occupied by the larger radius cation such as  $Sr^{2+}$ ,  $Ca^{2+}$ ,  $Ba^{2+}$ , and  $B$ -site cation was occupied by the smaller radius cation such as  $Ti^{4+}$ ,  $Nb^{5+}$ ,  $W^{6+}$ ,  $Ta^{5+}$  [2,3]. Some Aurivillius compounds that were reported to have good photocatalytic activity are  $Bi_2MO_6$  ( $M = W, Mo$ ) [4],  $Bi_4V_2O_{11}$  [5],  $Bi_2MO_5F$  ( $M = Nb, Ta$ ) [6],  $Bi_4Ti_3O_{12}$  [7].

$ABi_2Ta_2O_9$  ( $A = Ca, Sr, Ba$ ) are members of the two-layer compound Aurivillius, and some researchers reported its photocatalyst properties. Li et al. (2008) have reported that the bandgap energy of the two-layer  $ABi_2Ta_2O_9$  ( $A = Ca, Sr, Ba$ ) compound is 3.67, 3.64; 3.52 eV, respectively. They also measured the photocatalytic activity and reported that the compound  $ABi_2Ta_2O_9$  ( $A = Ca, Sr, Ba$ ) could produce  $H_2$  sequentially is 0.30, 2.26, and 0.11 mmol/h [8]. On the other hand, Senthil & Panigrahi (2019) reported a doped  $SrBi_2Ta_2O_9$  compound with yttrium element to enhance its photocatalytic activity [9].

Many researchers have synthesized  $ABi_2Ta_2O_9$  ( $A = Ca, Sr, Ba$ ) compounds using solid-state reaction (SSR). This method required higher calcination temperatures (about 1000-1200°C); thus, one of the disadvantages of solid-state reaction is agglomeration due to higher temperature conditions [10-12]. Pellegrino reported that the agglomeration particle affected photocatalytic activity because it can interfere with the process of photon radiation absorption [13]. Therefore the alternative synthesized method is needed as one strategy to enhance the photocatalytic activity of  $ABi_2Ta_2O_9$  ( $A = Ca, Sr, Ba$ ).

One synthesized methods that can produce the typical morphology is the molten salt method [14]. This method has the advantage, i.e., particle size and morphology control capability, avoid the agglomeration, simple equipment, requires low-temperature synthesis, short synthesis time [14-16]. Many researchers also reported that morphology

control is one technique to increase photocatalyst activity; thus, MSS gives a reasonable opportunity to gain a better photocatalyst material [17]. In this research, we have synthesized the  $ABi_2Ta_2O_9$  ( $A = Ca, Sr, Ba$ ) compound using the molten salts method. In addition, the samples obtained were further evaluated for photocatalyst activity in degrading the methylene blue solution.

## METHODOLOGY

Precursors used in the Synthesis of (a)  $CaBi_2Ta_2O_9$  (CBT) are  $CaCO_3$  (Sigma-Aldrich),  $Bi_2O_3$  (Sigma-Aldrich), and  $Ta_2O_5$  (Sigma-Aldrich), (b)  $SrBi_2Ta_2O_9$  (SBT) are  $SrCO_3$  (Sigma-Aldrich),  $Bi_2O_3$  (Sigma-Aldrich), and  $Ta_2O_5$  (Sigma-Aldrich), and (c)  $BaBi_2Ta_2O_9$  (BBT) are  $BaCO_3$  (Sigma-Aldrich),  $Bi_2O_3$  (Sigma-Aldrich), and  $Ta_2O_5$  (Sigma-Aldrich). All samples were synthesized using the molten salt method (The salt used is NaCl (Merck)). Precursors and salts with a ratio of 1:7 are weighed based on stoichiometric calculations and ground for 1 hour with added acetone, then calcined at temperatures of 700, 810, and 850°C for 6 hours.

All the samples were characterized using the X-ray diffraction technique (XRD) (Rigaku Miniflex diffractometer) to identify the phases formed. Measurement is performed in the range of  $2\theta$  ( $^\circ$ ) = 3-90. Particle morphology is characterized by scanning electron microscopy (SEM) (JEOL JSM-6360LA) and processed using Image-J software. The sample's optical properties are measured using ultraviolet-visible diffuse reflectance spectroscopy (UV-Vis-DRS) (Thermo Scientific Evolution 220 spectrometer) with a measurement range of 200-800 nm. The spectra obtained are calculated with the Kubelka-Munk equation to get the bandgap energy.

The photocatalytic activity evaluation was conducted by measuring the degradation of methylene blue. In this experiment, we used homemade photoreactors with a volume of 0.064 m<sup>3</sup> and commercial UV lamps as many as nine pieces. The evaluation began by inserting 100 ml of 6 ppm methylene blue solution into beaker glass and added CBT, SBT, and BBT catalysts of 0.1 grams. Then inserted into the photoreactor and stirrer for 30 minutes without light to ensure adsorption-desorption equilibrium takes place. The irradiation was done with a time variation of 0, 20, 40, 60, 80 minutes. After radiation is performed, the solution is let stand to precipitate the catalyst, and then measured the light absorption of the methylene blue using UV-Vis spectroscopy (Thermo Scientific Evolution 220 spectrometer).

## RESULT AND DISCUSSION

**Figure. 1** depicted the diffractograms of CBT, SBT, and BBT compounds and indexed using the Joint Committee on Powder Diffraction Standards (JCPDS) No. 490608 [8], and showed that some diffraction peaks correlated to identical peak diffraction of standard. It indicated that the target sample (CBT, SBT, and BBT) was successfully synthesized. However, additional peaks were still found that correlate to the impurities phase. The identification peaks result denote that the impurities phase is (a) in the  $CaBi_2Ta_2O_9$  sample found a  $CaBi_2O_4$  impurities phase identified by the diffraction peaks at  $2\theta$  ( $^\circ$ ): 33.58, 47.82, 48.79, (b) in the  $SrBi_2Ta_2O_9$  sample found a phase of impurities  $Ta_{0.703}O_{1.65}$  identified by the diffraction peaks at  $2\theta$  ( $^\circ$ ): 24.81, Phase of the  $TaO_{1.6}$  impurities identified by the diffraction peaks at  $2\theta$  ( $^\circ$ ): 51.71 and the impurities phase  $Sr_{0.19}Bi_{0.8}O_{1.4}$  identified by the existence of diffraction peak at  $2\theta$  ( $^\circ$ ): 52.55, (c) in  $BaBi_2Ta_2O_9$  sample found  $Ta_2O_5$  impurities phase identified with the diffraction peak at  $2\theta$  ( $^\circ$ ): 24.69,  $Bi_4O_7$  identified by the diffraction peaks at  $2\theta$  ( $^\circ$ ): 24.03, and  $TaO_{1.6}$  identified by the existence of diffraction peaks at  $2\theta$  ( $^\circ$ ): 27.74, 52.18. The impurities related to the difficulty in forming the Aurivillius phase with the molten salt method due to the ionic radii of cation-A (Ca, Sr, Ba) are longer than  $Bi^{3+}$  as results require the higher synthesis temperatures [18]. Some researchers successfully synthesized this compound by solid-state reaction method using higher temperatures, such as Li et al. (2008) using 1200 °C calcination temperature for 24 hours for CBT samples, SBT and BBT temperature 1000 °C for 72 hours [8].

Micrograph CBT, SBT, and BBT are shown in **Fig. 2**, and it can be seen that the particle samples shape is plate-like (varying size) and still found agglomerated particles. The plate-like form is well known as a typical morphology of the Aurivillius phase [19]. The measurement results of particle area and thickness are summarized in **Table 1**. The results showed that CBT, SBT, and BBT particles have a relatively large particle size range. Meanwhile, the agglomeration of particles is a consequence of the relatively rapid growth of crystals rather than nucleation formation. It is related to the usage of NaCl salts in the synthesis, which have low solubility [20].

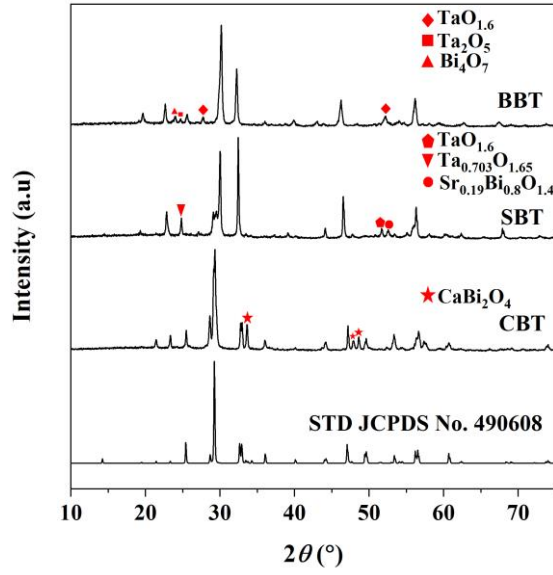
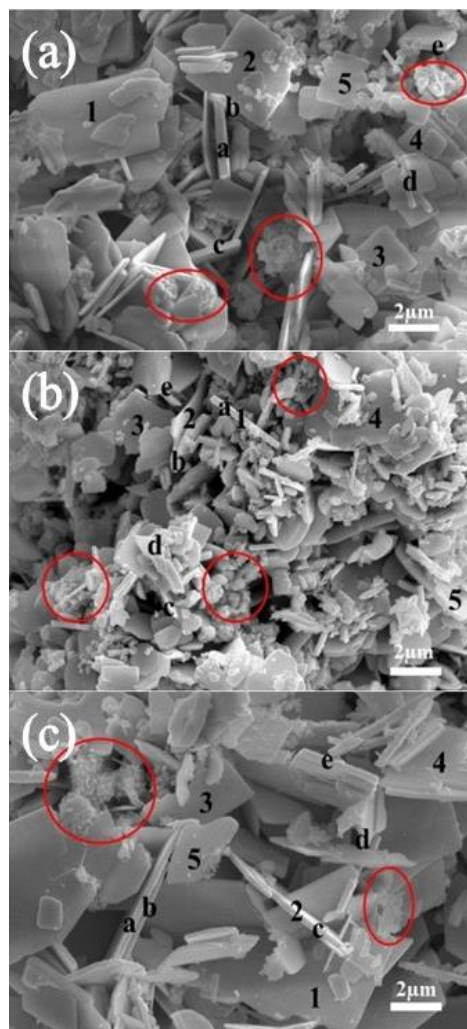


FIGURE 1. Diffractogram of CBT, SBT, and BBT

TABLE 1. CBT, SBT, and BBT particle sizes

Compound	Particle	Length ( $\mu\text{m}$ )	Width ( $\mu\text{m}$ )	Particle	Thickness ( $\mu\text{m}$ )
CBT	1	5.337	2.860	<i>a</i>	0.375
	2	3.455	3.125	<i>b</i>	0.263
	3	2.038	1.945	<i>c</i>	0.145
	4	2.353	1.384	<i>d</i>	0.152
	5	1.889	1.621	<i>e</i>	0.287
SBT	1	2.213	1.257	<i>a</i>	0.268
	2	2.092	1.741	<i>b</i>	0.174
	3	1.918	2.034	<i>c</i>	0.206
	4	2.897	2.643	<i>d</i>	0.198
	5	3.846	0.896	<i>e</i>	0.233
BBT	1	3.907	3.790	<i>a</i>	0.200
	2	4.370	1.172	<i>b</i>	0.251
	3	3.841	1.730	<i>c</i>	0.216
	4	2.549	2.221	<i>d</i>	0.173
	5	2.201	1.921	<i>e</i>	0.165

The bandgap energy was determined using the Kubelka-Munk equation with (a) CBT, and SBT used the direct-gap method, while BBT used the indirect-gap method [8, 21], and the Plot-Tauc calculation is depicted in Fig. 3. The result showed that the change of cation-A could decrease the bandgap energy and obtain a downward trend and the addition of the size of the atomic radius (Ca, Sr, Ba). The Investigating bandgap energy of  $ABi_2Ta_2O_9$  ( $A = \text{Ca, Sr, Ba}$ ) has been reported by Li et al. (2008). They suggested that the bandgap energy of the CBT, and SBT with orthorhombic structure, have similar bandgap energy of 3.67 and 3.64 eV. In contrast, BBT with a tetragonal structure is 3.52 eV [8]. The bandgap energy of CBT, SBT, and BBT compounds is affected by the electronic transition from conduction band (CB) to valence band (VB). The CB involved the electron in orbital Bi 6*p*, Ta 5*d*, and O 2*p*, while the VB involved the electron in orbital O 2*p*, Ta 5*d*, and Bi 6*s* [8].



**FIGURE 2.** The micrograph (a.) CBT, (b.) SBT, (c.) BBT. The red circle showed the agglomeration. The number and alphabet denote the particle which particle size and thickness calculated.

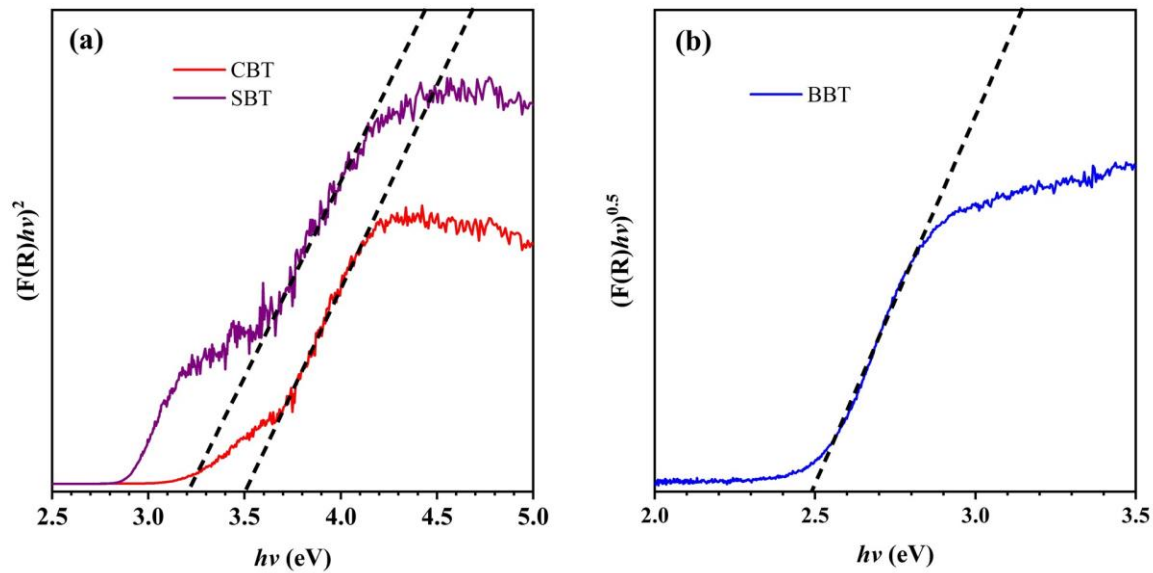


FIGURE 3. Plot-Tauc of (a) CBT, SBT (direct bandgap), and (b) BBT (indirect bandgap)

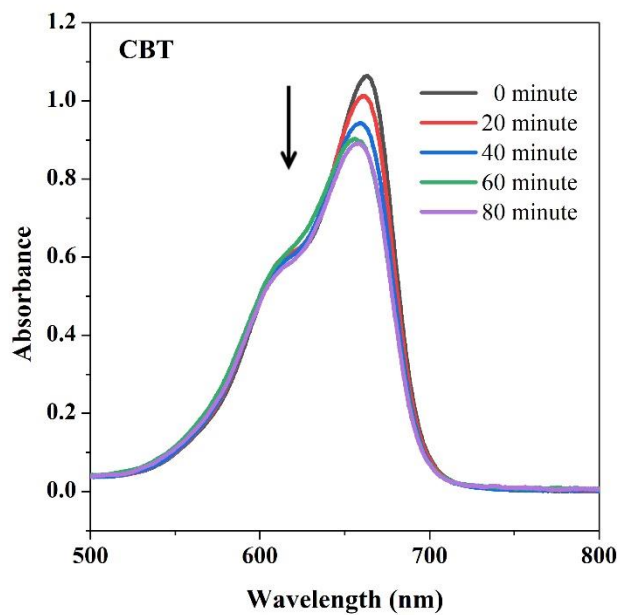


FIGURE 4. The degradation of methylene blue by CBT

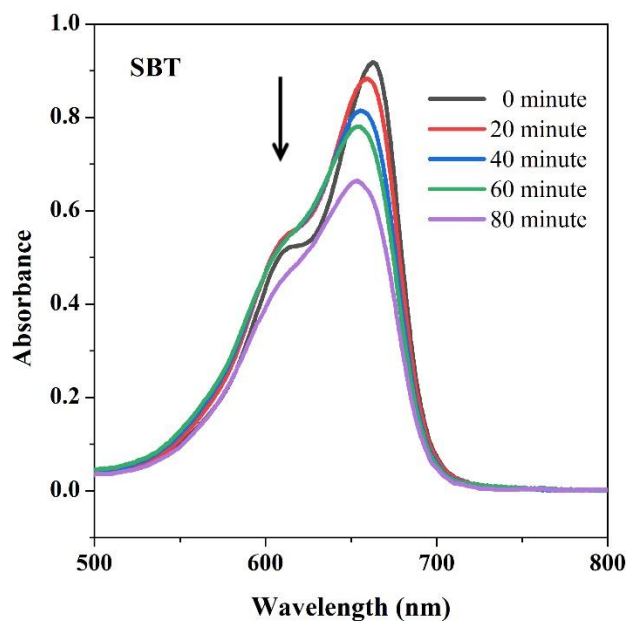


FIGURE 5. The degradation of methylene blue by SBT

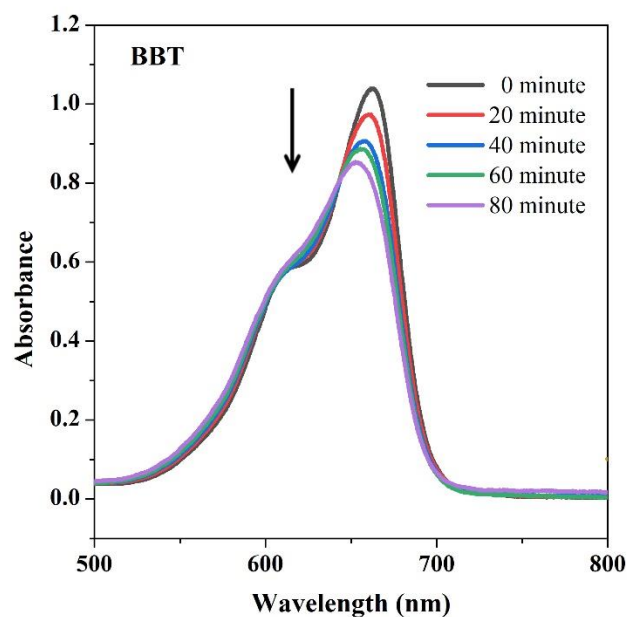
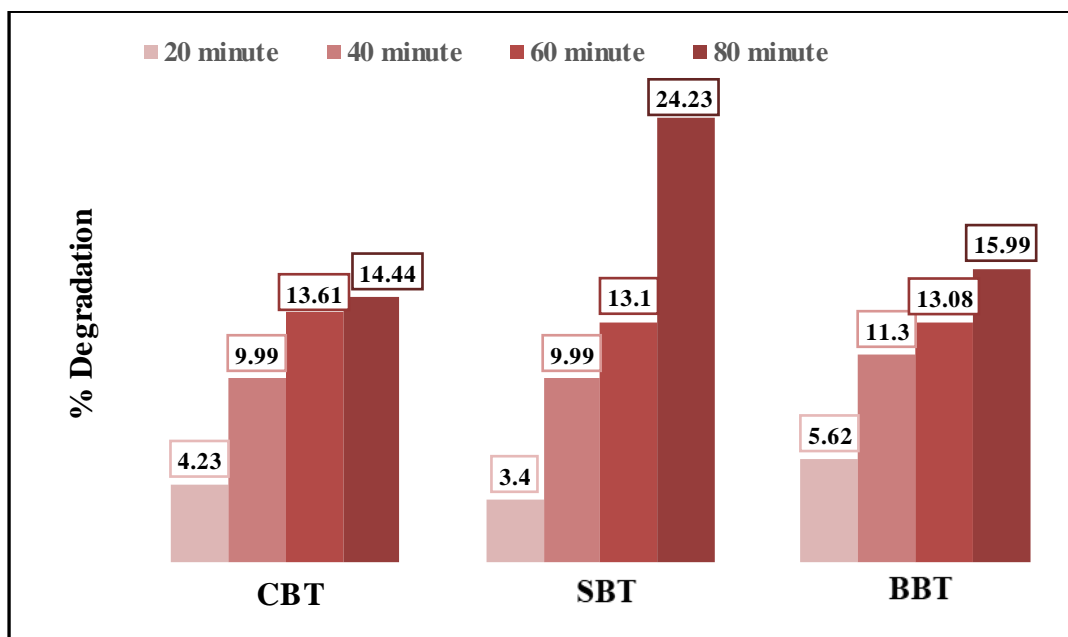


FIGURE 6. The degradation of methylene blue by SBT

Table 2. The energy value of the bandgap and wavelength of CBT, SBT, and BBT

Compound	Bandgap energy (eV)	Wavelength (nm)
CBT	3.51	353.23
SBT	3.21	386.24
BBT	2.44	508.13

The degradation evaluation results of methylene blue by CBT, SBT, and BBT are shown in **Figs. 4-6**. The percent degradation of CBT, SBT, and BBT compounds was depicted in **Fig. 7**. SBT samples have the highest degradation (24.2%) caused by uniform morphological form and fewer agglomeration particles than CBT and BBT. The photocatalytic reactions influence the surface area of material; thus, the smaller particle size (larger surface area) will have the higher photocatalytic activity [22-25]. Meanwhile, the agglomeration particle influences the depth of light radiation into the material. Thus the photocatalytic activity will decrease [13]. However, BBT (having the smallest bandgap energy) has a low photocatalytic activity (15.99%), and it may be related to the recombinant electron-hole rate. It is known that the smaller bandgap energy has a higher recombinant electron-hole rate [16]. However, the photoluminescence was not measured in this research; therefore, the effect of recombinant electron-hole to photocatalytic was not known.



**FIGURE 7.** Percent degradation of CBT, SBT, and BBT compounds against methylene blue

## CONCLUSION

CBT, SBT, and BBT materials have been successfully synthesized but found impurities. Plate-like particle morphology with a particle size of 2-5  $\mu\text{m}$  was formed with agglomeration. The bandgap energy of CBT, SBT, and BBT are 3.51, 3.21, and 2.44 eV, respectively. The photocatalyst activity in degrading methylene blue sequential is 14.44, 24.23, and 15.99% for 80 minutes.

## REFERENCES

1. Z.Z. Ding, X.Q. Tang, J.C. Ren, X.Z. Liu, Y.K. Chen, Z.Y. Xia, L. Cao, X.Q. Chen, and F.J. Yang, *Ceram. Int.* **46**, 8314 (2020).
2. L. Mi, Y. Feng, L. Cao, M. Xue, C. Qin, Y. Huang, L. Qin, and H.J. Seo, *J. Nanopart Res.* **20**, 2 (2018).
3. D. Wang, K. Tang, Z. Liang, and H. Zheng, *J. Solid State Chem.* **183**, 361 (2010).
4. C. Belver, C. Adán, and M. Fernández-García, *Catal. Today* **143**, 274 (2009).
5. Y. Lu, Y. Pu, J. Wang, C. Qin, C. Chen, and H.J. Seo, *Appl. Surf. Sci.* **347**, 719 (2015).
6. S. Lei, D. Cheng, X. Gao, L. Fei, W. Lu, J. Zhou, Y. Xiao, B. Cheng, Y. Wang, and H. Huang, *Appl. Catal. B Environ.* **205**, 112 (2017).
7. S. Li, X. Bian, J. Gao, G. Zhu, M. Hojamberdiev, C. Wang, X. Wei, *J Mater Sci: Mater Electron*, **28**, 17896–17907 (2017)
8. Y. Li, G. Chen, H. Zhang, Z. Li, and J. Sun, *J. Solid State Chem.* **181**, 2653 (2008).



9. V. Senthil and S. Panigrahi, *Int. J. Hydrog. Energy* **44**, 18058 (2019).
10. S. Marković, M. Mitrić, G. Starčević, and D. Uskoković, *Ultrason. Sonochem.* **15**, 16 (2008).
11. A. Thongtha, K. Angsukased, and T. Bongkarn, *Key Eng. Mater.* **421–422**, 247 (2009).
12. C. Kornpom, T. Udeye, and T. Bongkarn, *Integr. Ferroelectr.* **177**, 59 (2017).
13. F. Pellegrino, L. Pellutiè, F. Sordello, C. Minero, E. Ortel, V.-D. Hodoroaba, and V. Maurino, *Appl. Catal. B Environ.* **216**, 80 (2017).
14. T. Kimura, in *Advances in Ceramics - Synthesis and Characterization, Processing and Specific Applications*, edited by C. Sikalidis (InTech, 2011).
15. Y. Ishida, K.-I. Kakimoto, H. Ogawa, and M. Aki, *Ferroelectrics* **381**, 24 (2009).
16. Y. Liu, Y. Cao, H. Lv, S. Li, and H. Zhang, *Mater. Lett.* **188**, 99 (2017).
17. R. He, D. Xu, B. Cheng, J. Yu, W. Ho, *Nanoscale Horiz.* **3**, 464 (2018)
18. Zuhadjri, S.E. Afni, S. Arief, *Prosiding Semirata FMIPA Universitas Lampung*, 489-494, (2013)
19. Z. Zhao, X. Li, H. Ji, and M. Deng, *Integr. Ferroelectr.* **154**, 154 (2014).
20. H. He, W. Yao, C. Wang, X. Feng, and X. Lu, *Ind. Eng. Chem. Res.* **52**, 15034 (2013).
21. P. Makula, M. Pacia, and W. Macyk, *J. Phys. Chem. Lett.* **9**, 6814 (2018).
22. A.C. Dodd, A.J. McKinley, M. Saunders, and T. Tsuzuki, *J Nanopart Res* **8**, 43 (2006).
23. N. Xu, Z. Shi, Y. Fan, J. Dong, J. Shi, and M.Z.-C. Hu, *Ind. Eng. Chem. Res.* **38**, 373 (1999).
24. D. Li, H. Song, X. Meng, T. Shen, J. Sun, W. Han, and X. Wang, *Nanomaterials* **10**, 546 (2020).
25. T. Degabriel, E. Colaco, R. F. Domingos, K. E. Kirat, D. Brouiri, S. Casale, J. Landoulsi, and J. Spadavecchia, *Phys. Chem. Chem. Phys.* **20**, 12898-12907.